Research Article

Received: 9 June 2018 Revised: 17 October 2018 Accepted article published: 8 January 2019 Published online in Wiley Online Library: 21 February 2019

(wileyonlinelibrary.com) DOI 10.1002/jsfa.9564

Tea diseases detection based on fast infrared thermal image processing technology

Ning Yang,[a,b] Minfeng Yuan,[a] Pan Wang,[a] Rongbiao Zhang,[a*] Jun Sun[a] and Hanping Mao[b*]

ABSTRACT

BACKGROUND: As one of China's important economic crops, tea is economically damaged due to its large yield. The overall goal of this study is to develop an effective, simple, apt computer vision algorithm to detect tea disease area using infrared thermal image processing techniques and to estimate tea disease.

RESULTS: This paper finds that the area of tea disease has certain regularity with its infrared image gray distribution. Using this rule, we extracted two characteristic parameters into a classifier to help achieve rapid tea disease detection, which increases the accuracy of detection a small amount. The tea disease detection algorithm consisted of the following steps: classify canopy infrared thermal image; convert red, green and blue image to hue, saturation and value; thresholding; color identification; noise filtering; binarization; closed operation; and counting. A correlation coefficient R^2 of 0.97 was obtained between the tea disease detection algorithm and counting performed through human observation, which is 2% higher than traditional algorithms without classifiers.

CONCLUSIONS: This article provides guidance for monitoring the condition of tea gardens with airborne thermal imaging cameras.

Keywords: tea disease; infrared thermal image; image processing; fast classification; color detection

INTRODUCTION

Tea is one of the most popular drinks for Chinese people and is widely cultivated throughout China. As one of China's important cash crops, tea is exported and consumed in large quantities every year. As early as 2016, the area of tea gardens in China had reached 2.87×10^6 ha and the output was more than 2.4×10^6 tons. The scale of tea planting is the largest in the world, and the consumption exceeds 2×10^6 tons. However, tea diseases seriously affect the quality and result in one-fifth of the total yield of economic losses a year, increasing year by year with the increase of output.[1] One such serious disease is tea leaf blight, which results in a dry brown tea even in young tea plants and may kill the whole plant.[2] Therefore, the prevention and treatment of tea diseases, especially the early diagnosis and monitoring of tea diseases, is of great significance to production and quality decline.

At present, in actual production, peasants depend mainly on their own experience to diagnose crop diseases with their own senses.[3] However, most tea plants in China are planted in the mountains.[4] The large area of mountains brings greater difficulty and lower efficiency to field investigation. With the development of computer image processing technology, many methods based on image processing techniques have been proposed for use in agriculture. Amatya and Karkee developed an algorithm to detect cherry tree branches in dense foliage canopies by integration of visible branch sections and cherry clusters.[5] Beyaz *et al.* investigated a method to identify some Spanish olive cultivars using image processing techniques.[6] Zhang *et al.* demonstrated a new computer vision detection algorithm to detect defective apples using automatic lightness correction and a weighted relevance vector machine classifier.[7] However, image processing methods based on computer vision have limitations depending on the lighting conditions. Under strong light conditions, disease information is easily interfered with to form a wrong judgment. And computer vision technology does not work under low light conditions. Furthermore, the processing of visible light images requires calculation of a large amount of useless data, which is inefficient.

In order to overcome this limitation, a great number of detection algorithms based on infrared thermography have been proposed in recent years.[8] Egea *et al.* utilized aerial thermal imaging and infrared thermometry to assess a crop water stress index.[9] Chrétien *et al.* developed an algorithm to detect white-tailed deer based on infrared thermal remote sensing.[10] Barbedo *et al.* employed infrared thermal images to detect ticks in cattle and proposed an algorithm for quantifying the infestation.[11] According to the fact that the disease destroys the transpiration function of the plant

* *Correspondence to: R Zhang, School of Electrical and Information Engineering, Jiangsu University, Zhenjiang, China. E-mail: zrb@ujs.edu.cn; or H Mao, Agricultural Equipment Department, Jiangsu University, Zhenjiang, China. E-mail: yvincent2332@163.com*

a *School of Electrical and Information Engineering, Jiangsu University, Zhenjiang, PR China*

b *Institute of Agricultural Engineering, Jiangsu university, Zhenjiang, PR China*

and the relationship between the water content of the plant and the temperature, infrared thermal imaging technology indirectly obtains the disease condition of the plant by directly measuring the temperature of the plant leaf. However, the application of these infrared image technologies is carried out in a laboratory environment, with the aid of high-speed computing. In practical applications, in the early stage of the disease, only one or two of the 10 000 tea trees may be ill, far less than the number of healthy tea trees, which will cause a large amount of data redundancy, which is the same as the problem encountered with visible image processing. In addition, useless detection areas also reduce the accuracy of the detection.

In this study, we proposed a method using a tea disease rapid detection algorithm based on infrared thermal imaging technology. Tea plant images were taken from Jiangsu Tea Expo Park, China, at noon and camera shooting height was 2 m. The feature curve of grayscale distribution is analyzed and two important parameters are extracted to classify the canopy image quickly. The method is established by fast classification, color detection, grayscale processing, median filtering, binarization, closed operation, and other steps. Color segmentation is used to quickly detect tea disease areas, and closed operation effectively fills the holes created by wrong segmentation of the targets. These steps achieve rapid classification of canopy images and early detection of tea disease.

MATERIALS AND METHODS

Image acquisition and preprocessing

With the goal of developing and testing the proposed tea disease detection algorithm, a Fluke TiS20 infrared thermal camera was fixed to the pan\tilt\zoom at the bottom of the unmanned aerial vehicle (UAV). The images were captured in the 'auto-focus' mode. In July, the solar elevation angle in Zhenjiang, China, at 1 p.m. was about 81° and the local temperature was about 33 °C. Images were obtained by the UAV at a height of 2 m, and the algorithm was numerically simulated by computer. The algorithm will be later ported to a single-chip on the UAV. Lighting conditions have a major influence on the detection feasibility, and the most problematic factors occur with direct sunlight, which results in uneven temperature distribution. Such undesirable effects can be minimized by acquiring images under diffusive light conditions. Figure 1(a) provides a near-ground image of the tea field of the referred location and Fig. 1(b) is the infrared thermal image of Fig. 1(a).

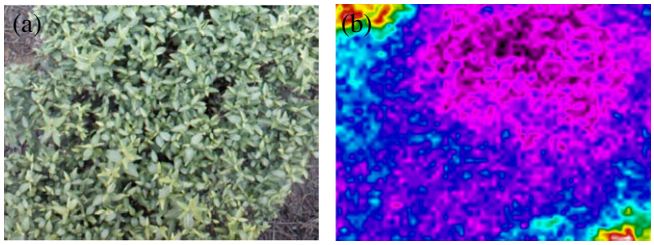

Figure 1. (a) Near-ground image of the tea field. (b) Infrared thermal image of the tea field.

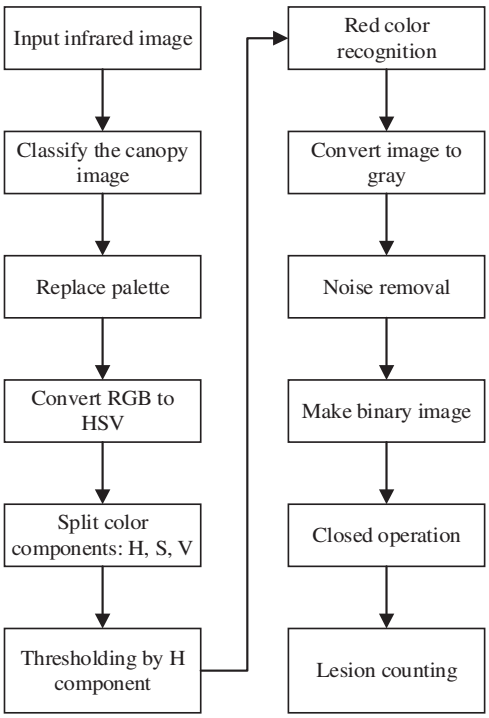

Figure 2. Flowchart algorithm of the overall methodology.

Image processing

The classes of original infrared thermal images of tea leaves include diseased yellow leaves, healthy green leaf, soil, trees, branches, and others. In order to classify and identify these images, we proposed a new algorithm flow chart, which is displayed in Fig. 2. The detection algorithm consists of the following steps: classification of canopy image, replace palette, converting red, green, and blue (RGB) images to hue, saturation, and value (HSV), split color components, thresholds, red color recognition, grayscale, noise removal, binarization, closed operation, and counting.

Classify the canopy image

Diseased images and healthy images are obtained from an infrared camera. Then these images are processed in the microcontroller. Prior to detecting the diseased leaf, we need to determine if the current area is likely to be a diseased area. We picked up three pictures of typical healthy areas and three pictures of typically diseased areas from 116 pictures obtained. Figure 3(a) is a picture of almost the entire healthy area in the window. The picture in Fig. 3(b) is of a half healthy area and half ground. Figure 3(c) is a picture of a healthy area and ground on both sides. Figure 3(d) shows a picture of a slightly diseased area. A picture of moderately diseased area is shown in Fig. 3(e). Figure 3(f) shows a picture of more seriously diseased area. Figure 4(a–f) are the respective grayscale distribution curves corresponding to Fig. 3(a–f).

Figure 4(a–c) shows the grayscale distribution curves of a healthy area. The main characteristic of the healthy area image is that pixels are basically concentrated in the low gray value range and other grayscale range has few pixels. Figure 4(d–f) shows the grayscale distribution curves of disease areas. We come to the conclusion from Fig. 4(d–f) that pixels in the diseased areas are uniformly distributed over the entire gray value range. Analyzing the gray distribution curves of the two types of images, we believe that there is a fixed threshold that can be used to distinguish between diseased areas and healthy areas. An unknown threshold T_0 is set, and we continuously optimize the threshold T_0 during the threshold segmentation of hundreds of infrared tea canopy

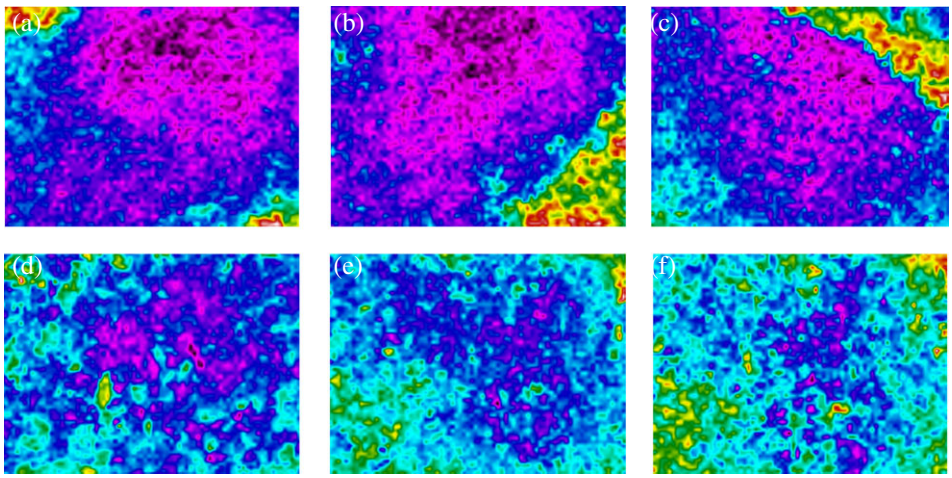

Figure 3. (a) – (c) Healthy area images; (d) – (f) diseased area images.

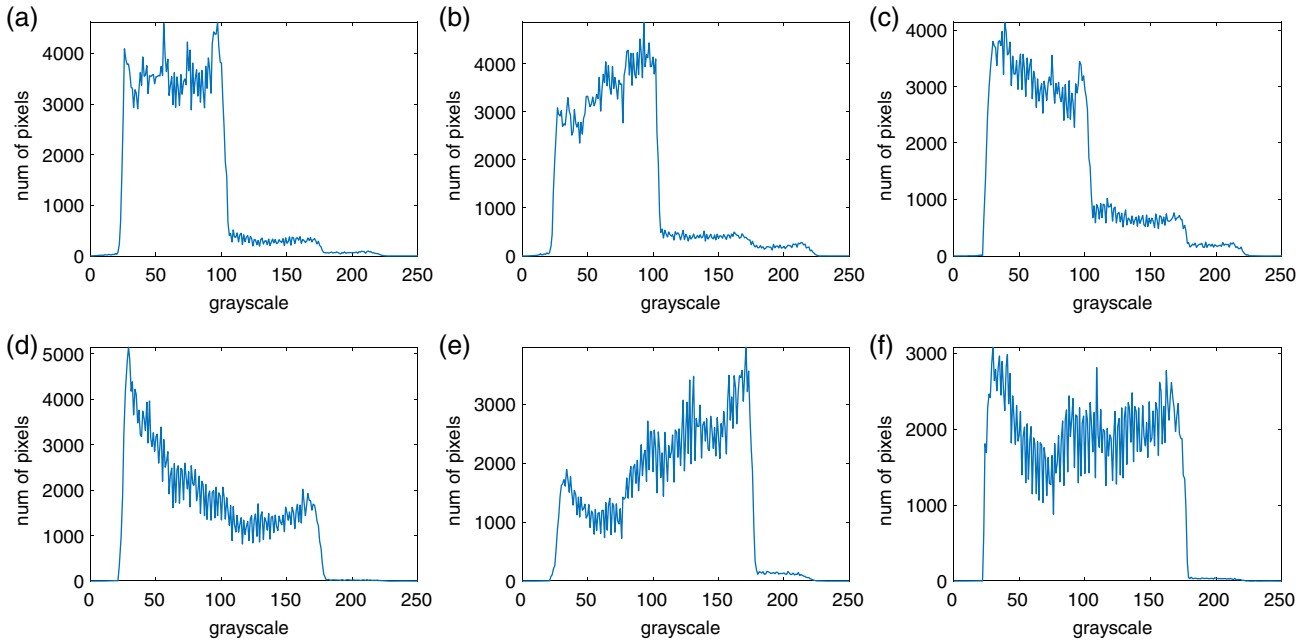

Figure 4. Grayscale graphs of: (a) – (c) healthy area images; (d) – (f) diseased area images.

images. Finally, we consider the proportion of pixels with a gray value less than 100 and the proportion of the dominant range as two future parameters for judging the healthy or diseased status of an area. It is worth mentioning that the threshold of 100 is relatively fixed in the experiments conducted in this paper, but will change to adapt to the climatic conditions, land conditions and tea types in other experiments.

Using these findings, we created a classifier to reduce the amount of useless data calculations. All these steps are shown in Fig. 5. A large number of canopy infrared thermal images are input to get the general rule and exclude the interference caused by other factors on the image. The number of canopy images is large and reaches the quantitative requirement. Feature images mainly include color features, texture features, shape features and spatial relationship features of images. Through the extraction of these features, we found that the grayscale histogram of infrared canopy images has a certain regularity. Analyzing the grayscale distribution curve, we choose the ratio of the gray value range of the main value to the total gray range and the ratio of the number of pixels in the decision interval to the total number of pixels as feature parameters. The first feature parameter R, the ratio of the gray value interval of the main value to the total gray interval, is calculated as follows, where x_i is the point where the gray distribution curve increases fastest and x_j represents the point where the gray distribution curve reduces fastest:

$$x_i = \max\left(a\left(j+1\right) - a\left(j\right)\right) \tag{1}$$

$$x_j = \max\left(a\left(j+1\right) - a\left(j\right)\right) \tag{2}$$

$$R = \frac{x_j - x_i}{255} \tag{3}$$

The second feature parameter P, the ratio of the gray value interval of the main value to the total gray interval, is calculated

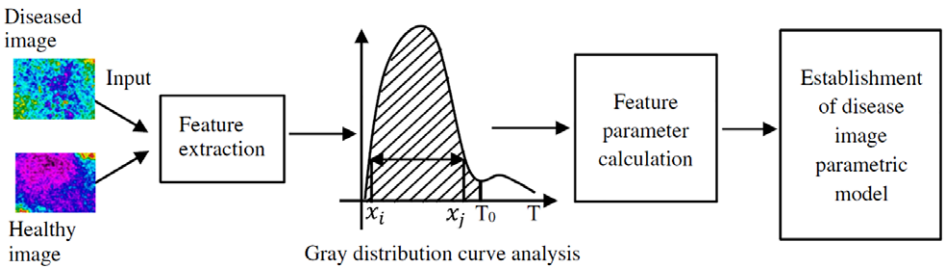

Figure 5. Canopy image classification diagram.

as follows, x and y stand for the number of length and width pixels respectively, S is the input image, and T is the grayscale value:

$$[x, y] = \text{size}(S) \tag{4}$$

$$P = \frac{\text{num}(T < 100)}{x \times y} \tag{5}$$

Based on these two feature parameters, we established a parametric model f of the disease image for later experimental applications. If input parameter P is between $P1$ and $P2$ and input R is between $R1$ and $R2$, we assume that the feature parameter is located in region A. This means the image has a parameter corresponding the a healthy tea plant image. Similarly, if input parameter P is between $P1'$ and $P2'$ and input R is between $R1'$ and $R2'$, we think the feature parameter is in region B, meaning a diseased plant image. These parameter thresholds $P1$, $P2$, $P1'$, $P2'$, $R1$, $R2$, $R1'$ and $R2'$ are obtained from the later experiments.

$$f = \begin{cases} A\,(\text{healthy}), & P1 < P < P2,\ \ R1 < R < R2 \\ B\,(\text{diseased}), & P1' < P < P2',\ \ R1' < R < R2' \end{cases} \tag{6}$$

Replace infrared thermal image palette and split color components

Color recognition is a key step in detecting disease. Therefore, the main features are extracted from the color information of pixels. The first step is to convert the color palette into a more appropriate one to make the detection task easier. In the default mode, the infrared camera uses iron red as the palette, which represents the temperature gradient in the saturation of red color. One drawback of using an iron red palette is the difficulty of having an objective threshold for color segmentation. High-contrast palettes use HSV color distribution to mark the image. This is conducive to image segmentation based on color threshold. We thus choose the high-contrast palette as the working mode.

The infrared camera saves pictures in RGB format, which indicates the intensity of the three primary colors (red, green, and blue). According to the principle of three primary colors of visible light, in the RGB color space, any visible light F can be a mixture of three basic colors of R, G and B in different proportions:

$$F = r[R] + g[G] + b[B] \tag{7}$$

This color model is based on simple additive composition, which is not completely intuitive from a perceptual point of view. One of the big shortcomings of using the RGB color space is the difficulty of separating the color information from the brightness. Instead of utilizing color primaries, HSV as a color description, as a more common gamut spatial transform, makes it easier for the algorithm to determine the range of processing to improve the accuracy of the algorithm. On the other hand, the color space of the HSV mode is consistent with the color palette of a high-contrast image, which helps to set the threshold for color recognition. This study uses only hue H for color recognition; saturation S and value V are no longer discussed.

The hue H of a color refers to which pure color it resembles, and is measured in terms of angles, with the range being from 0° to 360°. Viewing anticlockwise from the red, 0° is red, 120° is green and 240° is blue. Hue is calculated as follows:[12,13]

$$C_{\max} = \max\left(R', G', B'\right) \tag{8}$$

$$C_{\min} = \min\left(R', G', B'\right) \tag{9}$$

$$\Delta = C_{\max} - C_{\min} \tag{10}$$

$$H = \begin{cases} 60^\circ \times \left(\frac{G'-B'}{\Delta} mod 6\right), & C_{\max} = R' \\ 60^\circ \times \left(\frac{B'-R'}{\Delta} + 2\right), & C_{\max} = G' \\ 60^\circ \times \left(\frac{R'-G'}{\Delta} + 4\right), & C_{\max} = B' \end{cases} \tag{11}$$

Thresholding and red color detection

This study uses color information for image segmentation. Choosing an appropriate threshold is crucial for later color recognition. All image processing techniques are implemented in the spatial domain, which is a simple plane containing image pixels. The operation of the spatial domain can be provided by the following expression:

$$g(x, y) = T\left[f(x, y)\right] \tag{12}$$

Assuming that the grayscale histogram corresponds to an image $f(x, y)$ composed of dark targets in a light background, the grayscales of objects and background pixels are divided into two main modes. A simple way to extract an object from the background is to choose a threshold T to separate the models. Then, the point (x, y) in the image of $f(x, y) > T$ is called the target point, otherwise it is called the background point. In other words, the divided image $g(x, y)$ is given by the following expression:

$$g(x) = \begin{cases} 1, & \text{if } f(x, y) > T \\ 0, & \text{if } f(x, y) \le T \end{cases} \tag{13}$$

In the image processing we have proposed, the threshold divides the image into smaller lesion areas and larger background areas, and at least one color is used to define their boundaries.

Histogram-based methods are very simple and efficient over other image segmentation methods because they just require one value. For this technique, a histogram of color information is calculated for all the pixels in the image, and the image is divided into two levels of regions using the difference in color characteristics. Between the target regions, a more reasonable threshold is selected to determine whether a pixel belongs to the diseased area or background area.

Thresholding is made use of under the following conditions to have only lesion pixels in the images according to the H component: $h < 1/12$ (approximately 0.083). This value removes any healthy leaf and others from the image, and recognition with color components works well for the disease.

Convert RGB image to a gray image

We operate gray-scale processing on the image for the subsequent binarization step. Here, function $G(=\text{gray})$ converts an $R^{n\times m\times 3}$ color image into an $R^{n\times m}$ representation. Assume that all pixel values for images are between 0 and 1. R, G and B represent linear red, green, and blue channels respectively. The output of each grayscale algorithm is between 0 and 1. There are usually several existing algorithms that convert color images to grayscale. A common method uses a weighted combination of the RGB channels to produce a single gray value:[14]

$$G(=\text{gray}) = 0.2989 \times R + 0.5870 \times G(=\text{green}) + 0.1140 \times B \tag{14}$$

Noise removal

Unlike conventional visible light images that are processed by computer vision, infrared thermal images do not have to deal with complex background noise; the only need is to remove salt and pepper noise generated by signal pulses arising from the image sensors, transmission channels, and decoding processes. The common filtering methods are mean filtering, median filtering and Gaussian filtering. However, the averaging filter blurs the boundaries of the image. Gaussian filtering requires that the mean value of the image noise is zero, but the mean value of salt and pepper noise is not zero. Thus, the subsequent image processing operations are performed to remove such undesirable noise through median filtering.[15] The basic principle of median filtering is to replace the value of a point in a digital image with the median value of each point in a neighborhood of the point, so that the surrounding pixel values are close to the true value so as to eliminate isolated noise points. The method of median filtering employs a two-dimensional sliding template of a certain structure to sort the pixels in the board according to the pixel value and generates a monotonous rising (or falling) two-dimensional data sequence.

Produce a binary image

Binary images generate a lot of connected area for next lesion counting and have pixels with only two possible intensity values that are normally displayed as black and white. A grayscale or a color image is utilized to produce binary images for separating an object in the image from the background. The grayscale value smaller than the threshold becomes 0, and a value larger than the threshold becomes 1. The color of the object (usually white) is referred to as the foreground color. The rest (usually black) is called the background color. However, this polarity can be inverted depending on the image that is to undergo thresholding. When the polarity is inverted, the object is displayed with 0 and the background has a non-zero value. The binary image effectively segments higher temperature regions in the image.

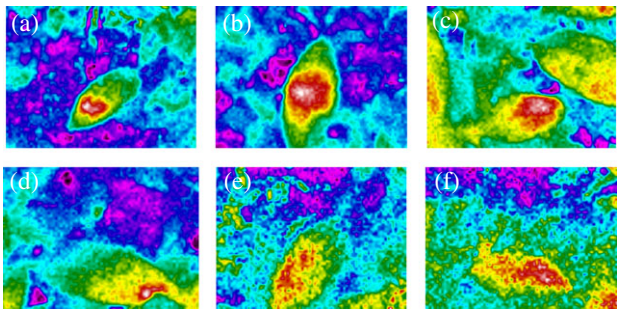

Figure 6. Single-leaf infrared thermal images.

Open–close operation

Owing to the shooting angle, many diseased leaves overlap, and so the images are incorrectly segmented in color recognition. In order to overcome this problem, we implement a closed operation on the segmented images to get close to the most realistic situation. X represents the target image and S stands for a structure element. The result of X's S erosion is the collection of all x that are still in X after the S is moved to X. In other words, the set obtained by using S to erode X is a set of S exactly where the origin of S is included in X, which is expressed as

$$X\Theta S = \{X|S + X \subseteq X\} \tag{15}$$

Dilation can be seen as a dual operation of erosion. The definition is that the structure element B is moved to a to get Ba, and if Ba hits X we take down this a point. All the sets of a points that meet the aforementioned conditions are called the results of the expansion of the X by the B:

$$X \oplus S = \left\{X|S + X \cup X \neq \emptyset\right\} \tag{16}$$

After dilation, erosion is called a closed operation. A closed operation can fill small holes and bridge small cracks, and the total position and shape are invariable:

$$X \cdot S = (X \oplus S)\Theta S \tag{17}$$

Lesion counting

We can count the number of connected areas to roughly determine the number of lesions. Healthy leaves usually overlapped other diseased leaves, which affected the disease estimation result to a certain extent. According to the combination result of previous segment of lesion, we could estimate the rank of the disease.

EXPERIMENTAL RESULTS AND DISCUSSION

Verification of the feasibility of infrared thermal imaging processing technology

Figure 6 illustrates single-leaf infrared thermal images. It is obvious from Fig. 6(a–f) that green is the healthy leaf, yellow is the infected region(not currently bad enough to be considered diseased) and red is the diseased region. These images indicate that the average temperature of the diseased (red-white) region is higher than the healthy (green) area, and the temperature of the infected

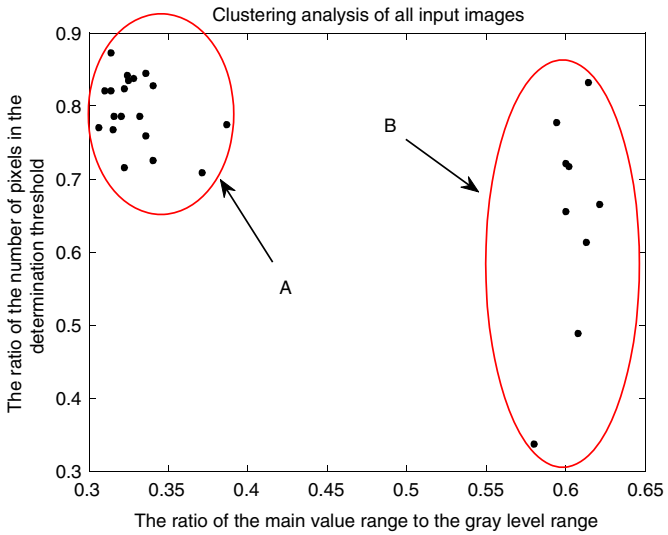

Figure 7. Clustering analysis of all input images.

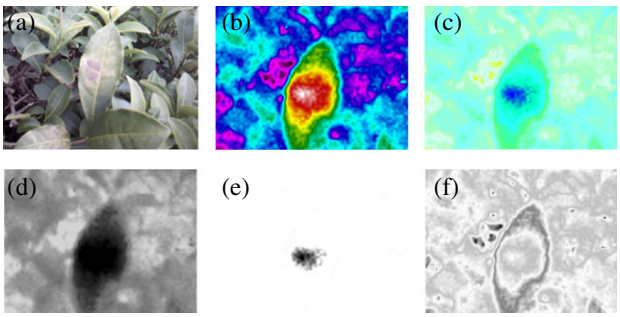

Figure 8. (a) Visible image; (b) input infrared thermal image; (c) HSV image of input infrared thermal image; (d) *H* panel image; (e) *S* panel image; (f) *V* panel image.

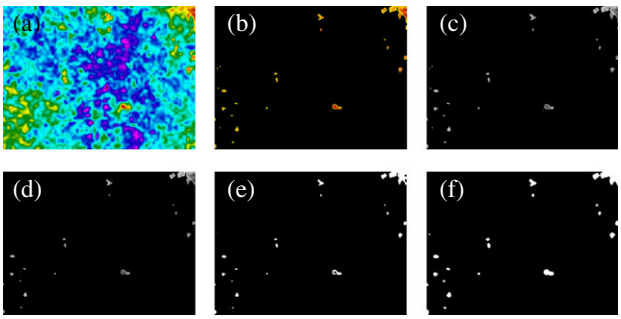

Figure 10. (a) Original image; (b) red color recognition; (c) red color changed to gray color; (d) noise removal image; (e) noise removal binary image; (f) closing operation.

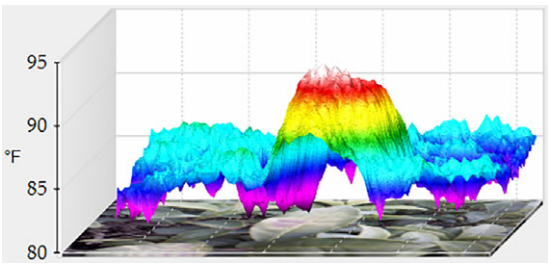

Figure 9. Three-dimensional infrared image.

(yellow) area is not as high as in the diseased region. Disease stress can be divided into the infection period, the incubation period and the onset period. In the infection period, various pathogens, like fungi, bacteria and viruses, infect the leaf surface and attack the stoma, leading to abnormal closure of stoma, which is used to adjust leaf temperature.[16] This is a reason why the temperature of a diseased region is higher than a healthy area. In the incubation period, pathogens multiply and spread in the host and fight with host plant. It can explain for the higher temperature of surrounding health area than other health area. In the onset period, pathogens massively multiply and increase harm. Therefore, we could recognize the disease area by detecting the yellow, red and white region.

Results of canopy image classification

We extracted the characteristic parameters for hundreds of infrared thermal images. A clustering analysis is shown in Fig. 7 depending on the two feature parameters. The parameter thresholds of the parameter model f are obtained from Fig. 7 and are displayed in Equation (18);

$$f = \begin{cases} A\,(\text{healthy}), & 0.6 < P < 1,\ \ 0 < R < 0.4 \\ B\,(\text{diseased}), & 0.55 < R < 1 \end{cases} \tag{18}$$

Region *A* represents a healthy tea image, where the proportion of the number of pixels in the determination threshold is >0.6 and the ratio of the main value range to the gray level range is <0.4. Region *B* represents a diseased tea image, where the ratio of the main value range to the gray level range is >0.55. An infrared thermal image takes only 20 ms to complete the classification operation. The result demonstrates the feasibility of quickly classifying the canopy image by extracting the two parameters.

Results of recognition algorithm

The main goal of this paper is to study the feasibility of detecting the lesion region on tea plants to estimate the degree of disease in those plants. The infrared thermal image of the diseased tea was detected by using the proposed algorithm and discussed the detection accuracy at the single leaf level. The results obtained,

Table 1. Disease detection results of green tea

Image	Count		Error (%)
	Observers	Algorithm	
01	48	51	6.25
02	19	17	−10.5
03	53	56	5.66
04	43	45	4.65
05	27	26	−3.70
06	39	38	−2.56
07	24	27	12.5
08	36	32	11.1
09	51	48	−5.89
10	43	44	2.33
11	35	37	5.71
12	15	13	−13.3
13	21	20	−5.00
14	45	43	−4.44
15	34	33	−2.94
16	57	54	−5.26
17	48	49	2.08
18	53	55	3.77
19	36	35	−2.78
20	50	52	4.00

from a total of 116 images from 57 tea plants, are shown in Fig. 8. Figure 8(a) shows a visible image with an obvious lesion, whose infrared thermal image is displayed in Fig. 8(b). Figure 8(c) illustrates an HSV image of Fig. 8(b) for subsequent color components splitting. The *H* panel image is shown in Fig. 8(d), which reflects the basic color of the image and is mainly utilized for color recognition. The *S* panel image is shown in Fig. 8(e) and the *V* panel image is displayed in Fig. 8(f). Figure 9 illustrates a three-dimensional infrared image and can be used to obtain a clear rule that the temperature of the red area is higher than other areas, proving the feasibility of color segmentation on disease areas.

The algorithm results for the canopy infrared thermal image are shown in Fig. 10. Figure 10(a) shows a remote-sensing infrared thermal image, and the result for red recognition is displayed in Fig. 10(b). Red areas and areas near red are considered as disease areas, whereas yellow is considered as an infected area, green is healthy area and blue is ground. Therefore, the red area and the area near red are preserved, and the other areas become black (the value is 0). A grayscale image is demonstrated in Fig. 10(c), which is used for binarization. Figure 10(d) is the noise removal image. It employs the nonlinear characteristics of the median filter to effectively filter salt and pepper noise caused by hardware imaging. Figure 10(e) is a binary image and Fig. 10(f) shows the image after the closing operation. In Fig. 10(f), because of the improper selection of the threshold, the originally connected region is incorrectly segmented. After the closing operation, the image can be corrected, so that the red areas and the red in the original image are basically the same. Finally, by using the recognition algorithm we can count 22 spots in Fig. 10(f). The whole calculation operation takes less than 35 ms and utilized half of the CPU.

Utilizing the algorithm proposed in this paper to detect the images obtained, we randomly selected 20 images; the simulation results analysis is displayed in Table 1 and Fig. 11(a). A regression analysis was conducted to compare the numbers of tea lesions counted by the new computer vision algorithm with those by direct human vision for the 116 images, as shown in Fig. 11(a).

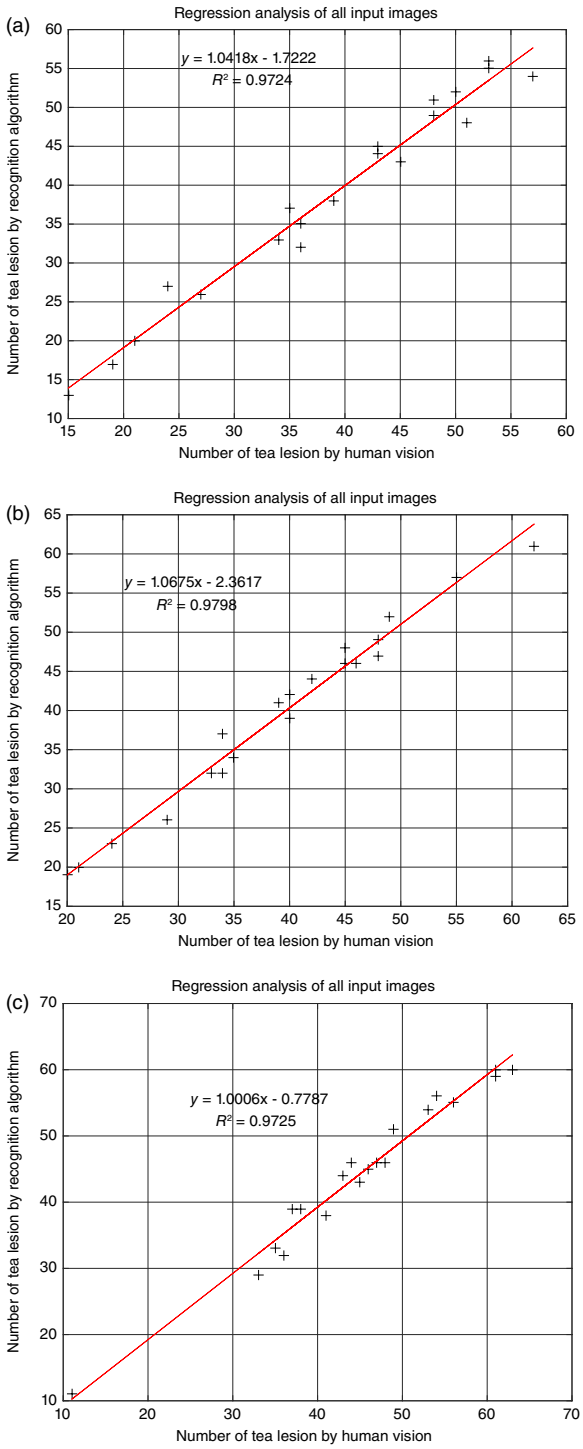

Figure 11. (a) Green tea; (b) white tea; (c) red tea.

The regression analysis value was of $R^2 = 0.97$. The tea we photographed belonged to green tea. As a control, we selected 20 more infrared images of white tea (Table 2, Fig. 11b) and 20 more infrared images of red tea (Table 3, Fig. 11c). From the analysis results, there are differences in the sensitivity of different types of tea to infrared thermal imaging, but from a numerical point of view it can be considered close. This parameter proves that using infrared thermal imaging technology to detect all kinds of tea is feasible and has high recognition accuracy.

Table 2. Disease detection results of white tea

Image	Count		Error (%)
	Observers	Algorithm	
01	33	32	−3.03
02	29	26	−10.3
03	49	52	6.12
04	62	61	−1.61
05	35	34	−2.86
06	39	41	5.13
07	34	37	8.82
08	46	46	0
09	45	48	6.67
10	40	39	−2.5
11	48	47	−2.08
12	20	19	−0.05
13	21	20	−4.76
14	45	46	2.22
15	24	23	−4.17
16	42	44	4.76
17	48	49	2.08
18	55	57	3.63
19	34	32	−5.88
20	40	42	0.05

Table 3. Disease detection results of red tea

Image	Count		Error (%)
	Observers	Algorithm	
01	36	32	−1.11
02	45	43	−4.44
03	61	59	−3.28
04	37	39	−5.41
05	53	54	5.89
06	46	45	−2.17
07	33	29	−12.1
08	44	46	4.55
09	63	60	−4.76
10	49	51	4.08
11	43	44	2.33
12	54	56	3.70
13	11	11	0.00
14	61	60	−1.64
15	47	46	−2.13
16	35	33	−5.71
17	41	38	−7.32
18	48	46	−4.17
19	56	55	−1.79
20	38	39	2.63

CONCLUSIONS

This paper developed a study on tea diseases detection based on fast classification of infrared thermal image processing. A grayscale distribution curve of the canopy image is calculated to create a classifier to achieve rapid classification of the disease image, which helps extend the working life of the UAV and greatly improves the accuracy of the detection. The algorithm consists of classification of canopy image, converting RGB images to HSV, thresholds, red recognition, noise removal, binarization, closed operation, and counting. The simulation output illustrates that the new counting algorithm was suitable and effective. A coefficient of determination R^2 of 0.97 is obtained between the lesion counting algorithm and counting performed through human observation.

ACKNOWLEDGEMENTS

This work was supported by National Natural Science Foundation of China (grant number 31701324), China Postdoctoral Science Foundation (grant number 2018M643182), Jiangsu Agricultural Science and Technology Innovation Fund (grant number CX(18)3043), and Outstanding Youth Foundation of Jiangsu Province of China (grant number BK20180099).

REFERENCES

1 Afzal M, Safer AM and Menon M, Green tea polyphenols and their potential role in health and disease. *Inflammopharmacology* **23**:151–161 (2015).
2 Pang J, Zhang TZ, Bassig BA and Mao C, Green tea consumption and risk of cardiovascular and ischemic related diseases: a meta-analysis. *Int J Cardiol* **202**:967–974 (2016).
3 Oz HS, Chronic inflammatory diseases and green tea polyphenols. *Nutrients* **9**:E561 (2017).
4 Pang J, Zhang Z, Zheng T, Yang YJ and Li N, Association of green tea consumption with risk of coronary heart disease in Chinese population. *Int J Cardiol* **179**:275–278 (2015).
5 Amatya S and Karkee M, Integration of visible branch sections and cherry clusters for detecting cherry tree branches in dense foliage canopies. *Biosyst Eng* **149**:72–81 (2016).
6 Beyaz A, Özkaya MT and İçen D, Identification of some Spanish olive cultivars using image processing techniques. *Sci Hortic* **225**:286–292 (2017).
7 Zhang B, Huang W, Gong L and Zhao C, Computer vision detection of defective apples using automatic lightness correction and weighted RVM classifier. *J Food Eng* **146**:143–151 (2015).
8 Fernández-Cuevas I, Marins JCB, Lastras JA, Carmona PMG and Cano SP, Classification of factors influencing the use of infrared thermography in humans: a review. *Infrared Phys Technol* **71**:28–55 (2015).
9 Egea G, Padilla- Díaz CM, Martinez-Guanter J, Fernández JE and Pérez-Ruiz M, Assessing a crop water stress index derived from aerial thermal imaging and infrared thermometry in super-high density olive orchards. *Agric Water Manag* **187**:210–221 (2017).
10 Chrétien L, Théau J and Ménard P, Visible and thermal infrared remote sensing for the detection of white-tailed deer using an unmanned aerial system. *Wildlife Soc B* **40**:181–191 (2016).
11 Barbedo JGA, Gomes CCG, Cardoso FF, Domingues R and Ramos JV, The use of infrared images to detect ticks in cattle and proposal of an algorithm for quantifying the infestation. *Vet Parasitol* **235**:106–112 (2017).
12 Kobalicek P and Bliznak M, Optimized RGB to HSV color conversion using SSE technology, in *Annals of DAAAM for 2011 & Proceedings of the 22nd International DAAAM Symposium*, ed. by Katalinic B. DAAAM International, Vienna, Austria, pp. 1591–1592 (2011).
13 Nishad PM and Manicka Chezian R, Various color spaces and color space conversion algorithms. *Journal of Global Research in Computer Science* **4**:44–48 (2013).
14 Nsfchi HZ., Shahkolaei A., Hedjam R., Cheriet M.. CorrC2G: color to gray conversion by correlation, in *IEEE Signal Proc Let* (**24**):1651–1655 (2017).
15 Matsuoka J, Koga T, Suetake N and Uchino E, Switching non-local median filter. *Opt Rev* **22**:448–458 (2015).
16 Behmann J, Mahlein AK, Rumpf T, Römer c and Plümer L, A review of advanced machine learning methods for the detection of biotic stress in precision crop protection. *Precision Agriculture* **16**:239–260 (2015).